Influence of the surface Si/buried oxide interface on extended defect evolution in silicon-on-insulator scaled to 300 Å

A. F. Saavedra,[a] J. Frazer, and K. S. Jones
Department of Materials Science and Engineering, SWAMP Center, University of Florida, Gainesville, Florida 32611

I. Avci, S. K. Earles, and M. E. Law
Department of Electrical and Computer Engineering, SWAMP Center, University of Florida, Gainesville, Florida 32611

E. C. Jones
IBM Semiconductor Research and Development Center, Research Division, Yorktown Heights, New York 10598

(Received 28 May 2002; accepted 3 September 2002)

As device dimensions continue to be scaled, incorporation of silicon-on-insulator (SOI) as mainstream complementary metal–oxide–semiconductor technology also increases. This experiment set out to further investigate the effect of the surface Si/buried oxide (BOX) interface on the formation and dissolution of extended defects in SOI. UNIBOND® wafers were thinned to 300, 700, and 1600 Å. Si^+ ion implantation was performed from 5 to 40 keV with a constant, nonamorphizing dose of 2×10^{14} cm^{-2}. Inert ambient furnace anneals were performed at 750 °C for times of 5 min up to 8 h. Transmission electron microscopy was used to study the evolution of extended defects, as well as to quantify the number of trapped interstitials. It is observed that the surface Si/BOX interface does not enhance the dissolution rate of extended defects unless $\geqslant$15% of the dose is truncated by the BOX. Further, no reduction in the trapped interstitial concentration is seen unless $\geqslant$6% of the dose is truncated. It is concluded that the surface Si/BOX interface does not serve as a significant sink for interstitial recombination, as long as the interstitial profile is mostly confined to the surface Si layer. © *2002 American Vacuum Society.* [DOI: 10.1116/1.1517410]

I. INTRODUCTION

Silicon-on-insulator (SOI) possesses a number of inherent advantages over traditional bulk silicon-based microelectronics. These include the elimination of latch up, improved radiation hardness, low-power consumption, and higher operating temperatures.[1] Only recently has SOI become an affordable option, as the yield and quality of SOI wafers has improved.[2] In order to scale SOI devices in the future, the diffusion phenomena that take place must be understood so that process simulators can be updated. In this study, the effect of the surface Si/buried oxide (BOX) interface on extended defect evolution is further examined at 10 and 40 keV implant energies.[3]

Dopant diffusion in SOI has previously been shown to be quite different from that of bulk silicon.[4–7] Pileup of boron at the surface Si/BOX interface has been observed,[4,6] but is strongly influenced by the implant energy.[4] However, dopants such as phosphorus exhibit depletion at the interface.[4] The mechanism by which the presence of the buried oxide affects the diffusion has yet to be determined. Transient-enhanced diffusion (TED) is one of the main challenges affecting the formation of ultrashallow junctions.[8,9] Extended defects, such as {311} defects and dislocation loops, are major contributing factors to the amount of TED that is observed in bulk silicon.[10] Thus, examining the effect the surface Si/BOX interface has on extended defect evolution in SOI should help explain some anomalies of dopant diffusion in SOI as well.

II. EXPERIMENT

Czochralski and UNIBOND® wafers (200 mm, {001}, 14–22 Ω cm) having a BOX thickness of 4000 Å were used in the experiment. The surface silicon layer of the SOI wafers was thinned using oxidation and etching from 1600 Å down to 670–688 and 299–305 Å, respectively. The surface Si layer thickness was monitored using a Rudolf dual wavelength ellipsometer. The wafers were then implanted with $^{28}Si^+$ ions at energies ranging from 5 to 40 keV and a constant dose of 2×10^{14} cm^{-2}. The implant conditions did not result in amorphization of any of the materials. Anneals were done in a quartz tube furnace with a nitrogen ambient at 750 °C for times ranging from 5 min up to 8 h. Plan-view transmission electron microscopy (PTEM) samples were prepared and imaging was done using a JEOL 200CX TEM operating at 200 kV. Images were taken using a $\mathbf{g}_{220}$ diffracted beam under $\mathbf{g}(3\mathbf{g})$ weak beam dark-field conditions. Finally, quantitative TEM (QTEM) was used to calculate the concentration of trapped interstitials (Si_I) in extended defects.

III. RESULTS

Figure 1 shows the interstitial concentration (C_I) profiles simulated using UT-Marlowe. This illustrates that as the implant energy increases and the surface Si thickness decreases,

[a]Electronic mail: asaav@ufl.edu

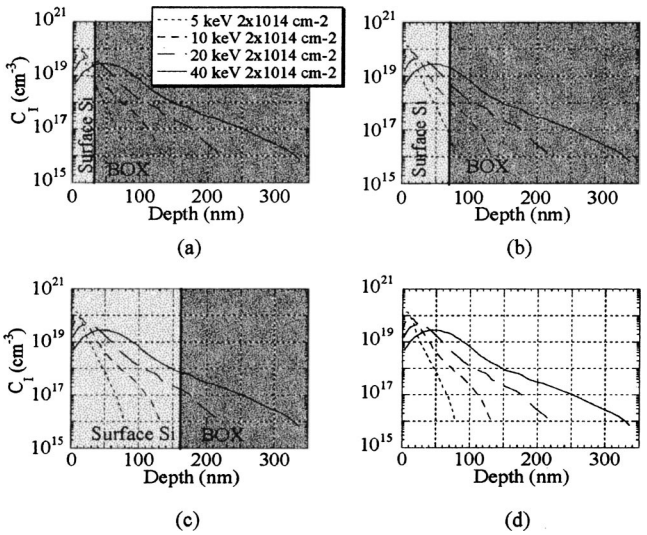

FIG. 1. Interstitial concentration (C_I) depth profiles from UT-Marlowe for (a) 300 Å, (b) 700 Å, (c) 1600 Å, and (d) bulk Si after Si^+ implantation from 5 to 40 keV 2×10^{14} cm^{-2}.

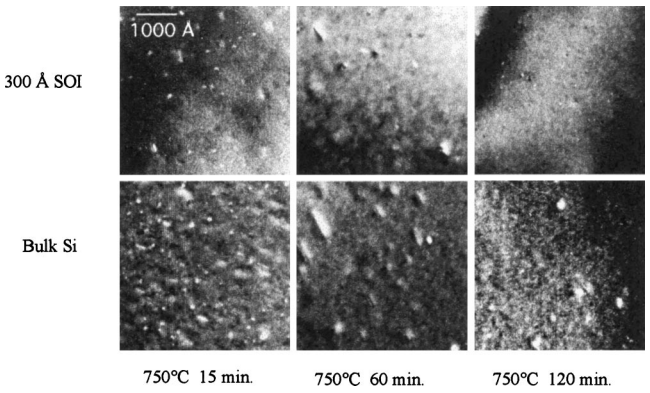

FIG. 3. Plan-view TEM micrographs illustrating defect evolution in 300 Å SOI and bulk Si for 5 keV, 2×10^{14} cm^{-2} after annealing at 750 °C (Ref. 3).

the concentration of interstitials in the BOX increases. Thus, fewer excess interstitials are available to aid in the formation of extended defects within the surface Si layer. Figure 2 shows the percent of dose retained in the surface Si layer as a function of implant energy. The 1600 Å SOI essentially receives the same dose as the bulk for all the implants, while the 700 Å SOI loses up to 25% at 40 keV. The 300 Å SOI loses approximately 45% and 80% at 20 and 40 keV, respectively.

Figures 3 and 4 show the PTEM micrographs and QTEM data, respectively, from Saavedra *et al.*[3] for the 5 keV samples. After annealing at 750 °C for 15 min, a combination of small interstitial clusters and zig-zag {311} defects can be seen in the 300 Å and bulk. The zig-zag {311} defects, which have been observed previously,[11] coarsen after annealing for 60 min. They begin to dissolve, as well as form small dislocation loops after 120 min. The dislocation loops appear much smaller in the 300 Å after 120 min, but the defect density is also much greater. As a result, the concentration of trapped interstitials in Fig. 4 is similar for each of the materials. Data for 5 keV, 3×10^{14} cm^{-2}, Si^+ implants from Agarwal *et al.*[11] is included for comparison.

The defect evolution for the 10 keV 300 Å SOI and bulk Si is shown in Fig. 5. At this energy, a larger portion of the dose ($\simeq$14%) is lost to the BOX compared to 5 keV. Thus, a decrease in the density of extended defects, as well as concentration of trapped interstitials occurs in the 300 Å SOI. There is also an increase in the size of the dislocation loops in bulk Si as implant energy increases. Close examination of the micrographs reveals the defects dissolve faster in the 300 Å SOI than the bulk. Quantification of the trapped interstitials (Fig. 6) shows a similar trend. A decrease in the concentration of trapped interstitials, as well as an increase in the dissolution rate occurs in the 300 Å. In addition, the decrease in Si_I is much greater than that predicted from the dose loss. However, the 700 and 1600 Å and bulk all behave similarly.

The 20 keV defect evolution for the 700 Å SOI and bulk Si are shown in Fig. 7 (from Saavedra *et al.*[3]). Dislocation loops appear to form from the unfaulting of {311} defects and the nucleation of the small interstitial clusters. Extended defects do not form in the 300 Å SOI due to the dose loss to the BOX. There appears to be a decrease in the defect size, as well as defect density in the 700 Å compared to the bulk. This would be expected due to the 6% dose loss at this energy. The concentration of trapped interstitials in Fig. 8 (from

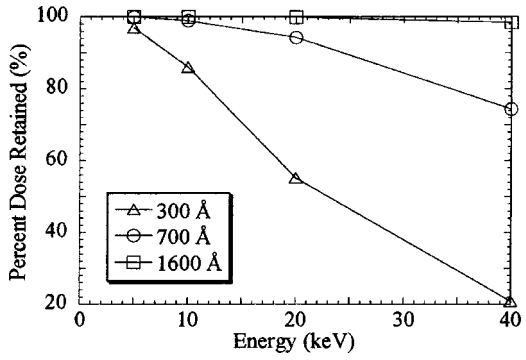

FIG. 2. Percentage of dose retained in surface Si layer of SOI for Si^+ implants from 5 to 40 keV, 2×10^{14} cm^{-2} (Ref. 3).

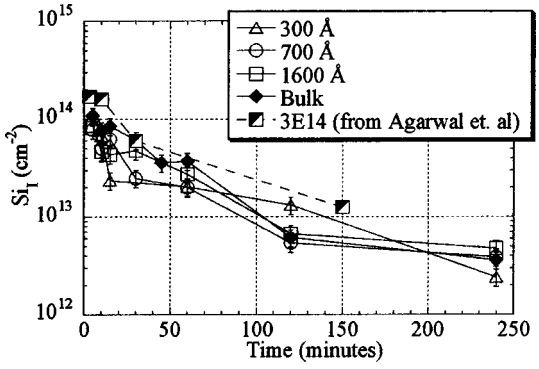

FIG. 4. Concentration of trapped interstitials (Si_I) in extended defects for 5 keV, 2×10^{14} cm^{-2} after annealing at 750 °C (Ref. 3).

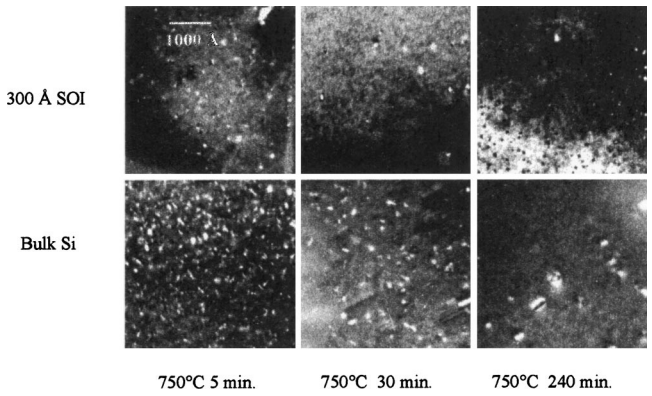

FIG. 5. Plan-view TEM micrographs illustrating defect evolution in 300 Å SOI and bulk Si for 10 keV, 2×10^{14} cm^{-2} after annealing at 750 °C.

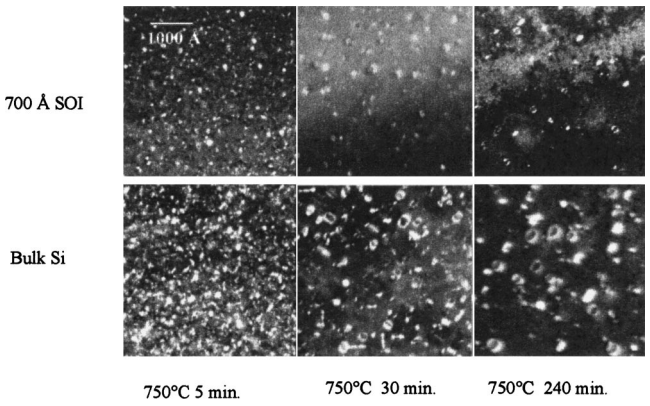

FIG. 7. Plan-view TEM micrographs illustrating defect evolution in 700 Å SOI and bulk Si for 20 keV, 2×10^{14} cm^{-2} after annealing at 750 °C (Ref. 3).

Saavedra *et al.*[3]) shows a similar trend. However, there is a larger decrease in trapped interstitials ($\simeq$35%) than predicted from the dose loss alone. In contrast, there is not an increase in the dissolution rate in the 700 Å. Overall, there is not a decay in the trapped interstitial concentration due to the stability of the dislocation loops at this energy.

Figure 9 shows the defect evolution for the 40 keV 700 Å SOI and bulk Si after annealing at 750 °C. Once again, a decrease in the defect size appears obvious in the 700 Å SOI, which could be attributed to the dose loss of 25%. The small dislocation loops in the 700 Å do not appear to coarsen, but rather appear to dissolve. The {311} defects begin to unfault and form dislocation loops after 30 min in the bulk samples. The dislocation loops are still present after annealing for up to 8 h. Figure 10 shows the QTEM data for the 40 keV samples. The 700 Å SOI exhibits a decrease in the concentration of trapped interstitials of approximately 95%, which is much larger than the 25% dose loss at 40 keV. There also appears to be an enhancement in the dissolution rate for the 700 Å. Like 20 keV, the 1600 Å SOI behaves similar to the bulk.

IV. DISCUSSION

The dissolution behavior for the 5 keV data set compares favorably with that done previously by Agarwal *et al.*[11] The surface Si/BOX interface does not appear to have a strong effect on recombination of trapped interstitials at this energy. This may be expected due to the projected range (100 Å) being furthest from the interface. However, there is a 5% dose loss in the 300 Å SOI, but there is not a detectable decrease in Si_I in Fig. 4. There have been a number of theories as to why there is an enhanced dissolution rate for low-energy compared to higher-energy Si^+ implants.[12–14] The presence of a higher supersaturation of excess interstitials may be the reason fewer extended defects are observed. Defects may not be able to trap as many interstitials due to the high supersaturation, creating a large flux into the crystal, rather than the surface being a dominant sink for interstitials.[15,16]

At 10 keV, the enhanced dissolution rate and decrease in Si_I in the 300 Å SOI is attributed to recombination at the surface Si/BOX interface. This is because the decrease in Si_I is much larger than the dose loss to the BOX. However, the fact that the other SOI samples behave similar to the bulk indicates that there is not an interface effect in thicker SOI at 10 keV.

For the 20 keV, a large decrease in Si_I for the 700 Å SOI is observed, but there is not an enhancement in the dissolu-

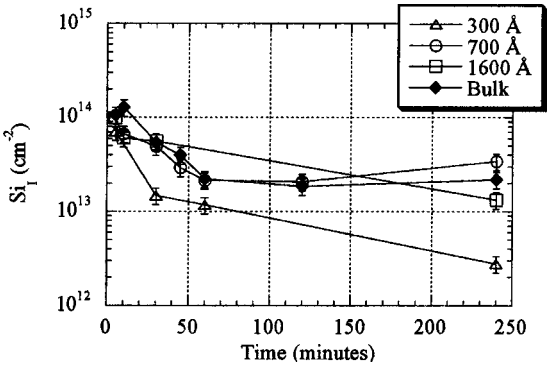

FIG. 6. Concentration of trapped interstitials in extended defects for 10 keV, 2×10^{14} cm^{-2} after annealing at 750 °C.

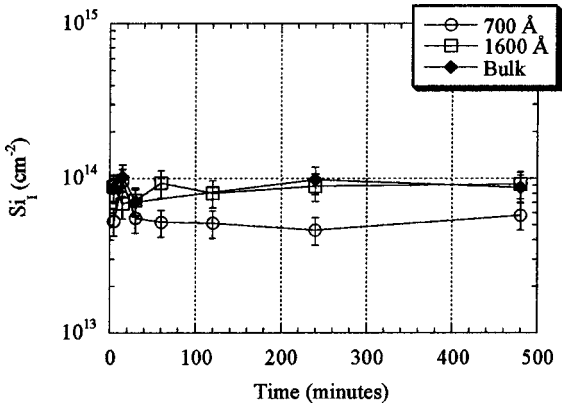

FIG. 8. Concentration of trapped interstitials in extended defects for 20 keV, 2×10^{14} cm^{-2} after annealing at 750 °C (Ref. 3).

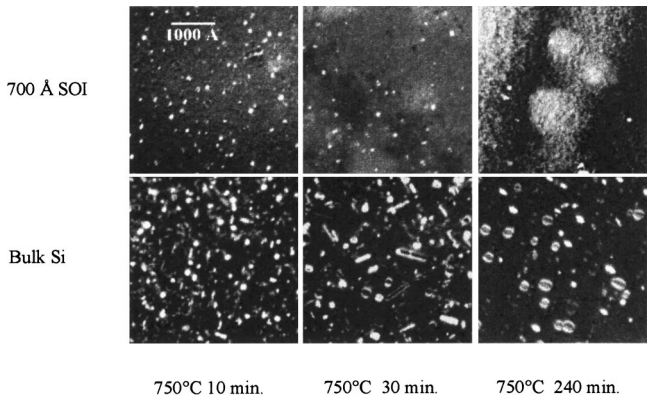

FIG. 9. Plan-view TEM micrographs illustrating defect evolution in 700 Å SOI and bulk Si for 40 keV, 2×10^{14} cm^{-2} after annealing at 750 °C.

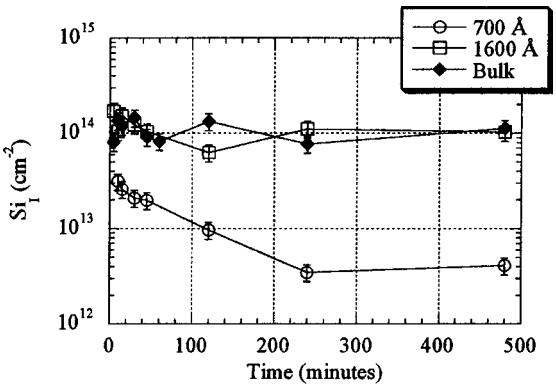

FIG. 10. Concentration of trapped interstitials in extended defects for 40 keV, 2×10^{14} cm^{-2} after annealing at 750 °C.

tion rate. This indicates that there is a dose loss threshold that must be exceeded before a decrease in Si_I can be quantified. This appears to occur around 6%.

An enhancement in the dissolution rate is observed for the 700 Å SOI at 40 keV. This indicates there is also a threshold for dose loss before an enhancement in the dissolution rate is observed. This threshold is approximately 15% since the 300 and 700 Å SOI show enhancement above 15%, but do not below 15%. There may also be a threshold for the formation of extended defects in SOI at the 2×10^{14} cm^{-2} dose. This is between 30% and 45% since no extended defects formed in the 300 Å at 20 keV (45% dose loss) and the extended defects were very small in the 700 Å at 40 keV (25% dose loss). However, this threshold is expected to vary depending on the implanted dose.

A number of theories have been proposed for the recombination of interstitials at a Si/SiO_2 interface.[17–20] As an interstitial approaches the Si/SiO_2 interface it may do a number of things: recombine along kink sites, diffuse into the oxide, react with the oxide, etc. Di-interstitial recombination[12] and formation of silicon monoxide[15] have been used to account for a wide range of experimental data. Production of SiO from the reaction $2Si+SiO_2\rightarrow2\,SiO$ has been used to account for the significant diffusivity of self-interstitials in silicon dioxide.[21] Enhanced and retarded diffusion of certain dopants due to a vacancy supersaturation has also been attributed to SiO.[22,23] However, the production of SiO is a high-temperature process and is unlikely to form under the annealing conditions used in this study.[21]

There appears to be one requirement for interstitial recombination to take place at the surface Si/BOX interface—dose loss to the BOX. Since the Si/SiO_2 interface is typically a very smooth interface for thicker thermally grown oxides,[24] it is a logical conclusion that the interface must be damaged in order to serve as a sink for trapped interstitials. This damage occurs whenever the implant profile is truncated by the BOX. By increasing the number of kink sites and dangling bonds at the interface, it is proposed the interstitials have a greater probability of recombining at the surface Si/BOX interface. However, without the damage the interface is unable to compete with the ability of extended defects to trap interstitials.

An alternative explanation is that the peak interstitial concentration must be within 100–200 Å of the interface before the trapped interstitial population is affected. However, the straggle of the implant is a more important parameter for this argument. At 20 keV, there is a noticeable decrease in Si_I for the 700 Å SOI, yet the peak interstitial concentration is 350–400 Å from the surface Si/BOX interface. The straggle is much greater at this energy. This could explain why there is not a decrease in Si_I for the 300 Å SOI at 5 keV. The peak interstitial concentration is only $\simeq$200 Å from the interface, but the straggle is much less at this energy so there is no noticeable decrease in Si_I. In order to place the peak interstitial concentration close to the interface the straggle must increase, thus more of the implant is truncated by the BOX leading to a damaged surface Si/BOX interface. This supports the proposition in the preceding paragraph.

V. CONCLUSIONS

The effect of the surface Si/BOX interface on extended defect evolution in SOI scaled to 300 Å has been investigated via plan-view TEM. It is observed that the interface does not enhance the dissolution rate of extended defects unless $\geqslant$15% of the dose is truncated by the BOX. Further, no reduction in the trapped interstitial concentration is seen unless $\geqslant$6% of the dose is truncated. It is concluded that the surface Si/BOX interface does not serve as a significant sink for interstitial recombination, as long as the interstitial profile is mostly confined to the surface Si layer. It is proposed that by effectively damaging the surface Si/BOX interface as the implant energy increases, the number of kink sites and dangling bonds are increased and the interstitials have a greater probability of recombining at the interface. Without the damage, the interface is unable to compete with the ability of the extended defects to trap interstitials. We will attempt to model the interface in the future in order to extract the recombination velocity of trapped interstitials.

ACKNOWLEDGMENTS

The efforts of the Advanced Si Technology Laboratory at the IBM T. J. Watson Research Center are greatly appreciated. This work was supported by the Semiconductor Research Corporation (SRC) under Task No. 819.001.

[1]J. P. Colinge, *Silicon-on-Insulator Technology: Materials to VLSI*, 2nd ed. (Kluwer Academic, Boston, MA, 1997), pp. 1–4.
[2]H. J. Hovel, Proceedings of the IEEE International SOI Conference (1996), p. 1.
[3]A. F. Saavedra, J. Frazer, D. Wrigley, K. S. Jones, I. Avci, S. K. Earles, M. E. Law, and E. C. Jones, Mater. Res. Soc. Symp. Proc. **717**, 95 (2002).
[4]H. Park, E. C. Jones, P. Ronsheim, C. Cabral, Jr., C. D'Emic, G. M. Cohen, R. Young, and W. Rausch, Tech. Dig. - Int. Electron Devices Meet. 337 (1999).
[5]H. Uchida, Y. Ieki, M. Ichimura, and E. Arai, Jpn. J. Appl. Phys., Part 2 **39**, L137 (2000).
[6]H.-H. Vuong, H.-J. Gossmann, L. Pelaz, G. K. Celler, D. C. Jacobson, D. Barr, J. Hergenrother, D. Monroe, V. C. Venezia, C. S. Rafferty, S. J. Hillenius, J. McKinley, F. A. Stevie, and C. Granger, Appl. Phys. Lett. **75**, 1083 (1999).
[7]S. W. Crowder, C. J. Hsieh, P. B. Griffin, and J. D. Plummer, J. Appl. Phys. **76**, 2756 (1994).
[8]E. C. Jones and E. Ishida, Mater. Sci. Eng., R. **24**, 1 (1998).
[9]P. A. Stolk, H.-J. Gossmann, D. J. Eaglesham, D. C. Jacobson, C. S. Rafferty, G. H. Gilmer, M. Jaraiz, J. M. Poate, H. S. Luftman, and T. E. Haynes, J. Appl. Phys. **81**, 6031 (1997).
[10]D. J. Eaglesham, P. A. Stolk, H.-J. Gossmann, and J. M. Poate, Appl. Phys. Lett. **65**, 2305 (1994).
[11]A. Agarwal, T. E. Haynes, D. J. Eaglesham, H.-J. Gossmann, D. C. Jacobson, J. M. Poate, and Yu. E. Erokhin, Appl. Phys. Lett. **70**, 3332 (1997).
[12]D. R. Lim, C. S. Rafferty, and F. P. Klemens, Appl. Phys. Lett. **67**, 2302 (1995).
[13]H. Saleh, M. E. Law, S. Bharatan, K. S. Jones, V. Krishnamoorthy, and T. Buyuklimanli, Appl. Phys. Lett. **77**, 112 (2000).
[14]K. Moller, K. S. Jones, and M. E. Law, Appl. Phys. Lett. **72**, 2547 (1998).
[15]M. Omri, C. Bonafos, A. Claverie, A. Nejim, F. Cristiano, D. Alquier, A. Martinez, and N. E. B. Cowern, Nucl. Instrum. Methods Phys. Res. B **120**, 5 (1996).
[16]A. C. King, A. F. Gutierrez, A. F. Saavedra, and K. S. Jones, J. Appl. Phys. (submitted).
[17]S. T. Dunham, J. Appl. Phys. **71**, 685 (1992).
[18]M. E. Law, Y. M. Haddara, and K. S. Jones, J. Appl. Phys. **84**, 3555 (1998).
[19]M. E. Law, IEEE Trans. Comput.-Aided Des. **10**, 1125 (1991).
[20]D. Tsoukalas, C. Tsamis, and J. Stoemenos, Appl. Phys. Lett. **63**, 3167 (1993).
[21]G. K. Celler and L. E. Trimble, Appl. Phys. Lett. **54**, 1427 (1989).
[22]S. T. Ahn, H. W. Kennel, W. A. Tiller, and J. D. Plummer, J. Appl. Phys. **65**, 2957 (1989).
[23]G. K. Celler and L. E. Trimble, Appl. Surf. Sci. **39**, 245 (1989).
[24]M. Bruel, B. Aspar, and A.-J. Auberton-Herve, Jpn. J. Appl. Phys., Part 1 **36**, 1636 (1997).